

T. Rodt
P. Ratiu
H. Becker
S. Bartling
D.F. Kacher
M. Anderson
F.A. Jolesz
R. Kikinis

3D visualisation of the middle ear and adjacent structures using reconstructed multi-slice CT datasets, correlating 3D images and virtual endoscopy to the 2D cross-sectional images

Received: 15 April 2001
Accepted: 7 January 2002
Published online: 7 August 2002
© Springer-Verlag 2002

T. Rodt · P. Ratiu · D.F. Kacher
M. Anderson · F.A. Jolesz
R. Kikinis (✉)
Surgical Planning Laboratory,
Brigham and Women's Hospital,
Harvard Medical School,
75 Francis Street,
02115 Boston MA, USA
E-mail: Kikinis@bwh.harvard.edu
Tel.: +1-617-7327389
Fax: +1-617-5826033

T. Rodt · H. Becker · S. Bartling
Department of Neuroradiology,
Hanover Medical School,
Hanover, Germany

Abstract The 3D imaging of the middle ear facilitates better understanding of the patient's anatomy. Cross-sectional slices, however, often allow a more accurate evaluation of anatomical structures, as some detail may be lost through post-processing. In order to demonstrate the advantages of combining both approaches, we performed computed tomography (CT) imaging in two normal and 15 different pathological cases, and the 3D models were correlated to the cross-sectional CT slices. Reconstructed CT datasets were acquired by multi-slice CT. Post-processing was performed using the in-house software "3D Slicer", applying thresholding and manual segmentation. 3D models of the individual anatomical structures were generated and displayed in different colours. The display of relevant anatomical and pathological structures was evaluated in the

greyscale 2D slices, 3D images, and the 2D slices showing the segmented 2D anatomy in different colours for each structure. Correlating 2D slices to the 3D models and virtual endoscopy helps to combine the advantages of each method. As generating 3D models can be extremely time-consuming, this approach can be a clinically applicable way of gaining a 3D understanding of the patient's anatomy by using models as a reference. Furthermore, it can help radiologists and otolaryngologists evaluating the 2D slices by adding the correct 3D information that would otherwise have to be mentally integrated. The method can be applied to radiological diagnosis, surgical planning, and especially, to teaching.

Keywords Middle Ear · Temporal Bone · 3D images · Virtual endoscopy · CT

Introduction

Understanding the complex anatomy of the middle ear and adjacent structures proves difficult by looking at cross-sectional 2D computed tomography (CT) images alone [1, 2, 3]. A 3D understanding of the individual anatomy is even more difficult to comprehend in the cases of implants or pathological conditions, such as malformation, trauma or tumour [3, 4, 5]. Mental integration of the 2D images can be even more difficult when the images are reconstructed to a small field of view (FOV), preventing direct comparison with the

contralateral side. With the increasing number of slices, when reconstruction is performed, the process of integrating them into a conceptual 3D model of the whole volume becomes even more difficult. On the other hand, reconstructed images allow a more detailed evaluation of the patient's anatomy or pathological condition [6]. Three-dimensional visualisation has been shown to facilitate the process of mentally stacking up the numerous 2D images in order to reach a thorough understanding of the patient's individual anatomy [3, 7, 8].

Three-dimensional visualisation of the temporal bone has been used for radiological diagnosis, surgical

planning, and teaching [2, 3, 5, 9, 10, 11, 12]. Various studies have been performed over the past years applying different algorithms of data acquisition and post-processing, depending on the diagnostic focus [4, 7, 13, 14, 15, 16, 17, 18, 19, 20]. Few of these algorithms are applied as a generally accepted clinical routine examination, since the procedure is time-consuming, and the computational means are not widely available. Furthermore, there have been few attempts to present standardised examination algorithms that could be adopted by institutions without experience in the 3D visualisation of the temporal bone.

All studies published on 3D visualisation of the temporal bone suggest it be used as a complementary examination, thereby indicating that 2D images still have advantages. Among these advantages is certainly the higher quality of display of the detail of the anatomy, as some of it is lost through the post-processing of the

original datasets [3]. Several of these studies, however, also showed that there is an indication for 3D visualisation in certain pathological conditions. To date, the 2D images and 3D visualisation have mostly been treated as independent examination modalities. A better correlation of these modalities might enhance the value of both the 2D images and the 3D visualisation for radiological diagnosis, surgical planning, and teaching.

Materials and methods

Low-dosage CT scans of 17 patients in the Department of Otorhinolaryngology, Hanover Medical School, Germany were obtained (see Table 1). The patients were 4 to 79 years of age (MV 30.94, SD 23.65 years). Seven patients were female and ten male. In seven cases the left petrous bone was investigated, in ten cases the right petrous bone. In patients 1 and 2, who had a pathological condition on the contralateral side, the middle ear was investigated

Table 1. Examined patients

Patient	Age (years)	Gender	Side	Diagnosis	Correlation of 2D slices to 3D images – findings of clinical relevance
1	27	Male	Left	Normal (cholesteatoma on the right)	(Figs. 1, 2, 3)
2	28	Male	Right	Normal (mastoiditis on the left)	–
3	10	Female	Right	Atresia of external acoustic meatus, aplasia of manubrium mallei	Meatal atresia and aplasia of manubrium shown, mandibular joint normal
4	16	Male	Left	Dysplastic long process of incus, atypical course of facial nerve	Abnormal superior course of dysplastic long process towards the stapes
5	32	Male	Right	Fracture of temporal bone running through cochlea	Spatial relationship of fracture and cochlea is displayed, continuity of ossicular chain is shown (Figs. 11, 12)
6	27	Male	Right	Dislocation of incudomalleolar joint	Discontinuity of ossicular chain is shown (Figs. 13, 14)
7	31	Male	Right	Fracture of temporal bone, dislocation of incudomalleolar and incudostapedial joint	Course of fracture, impingement of fracture fragment and discontinuity of ossicular chain are shown
8	54	Male	Right	Total ossicular replacement	Discontinuity of prosthesis and inner ear is shown
9	27	Female	Right	Stapes prosthesis	Continuity of ossicles and prosthesis between tympanic membrane and oval window is shown (Figs. 9, 10)
10	7	Female	Right	Cochlear implant	Spatial relationship of facial nerve and cochlear implant is displayed
11	15	Female	Left	Cochlear implant	Electrode is shown in cochlea, insertion of electrode through the basilar turn fenestration is visible (Figs. 4, 5)
12	4	Female	Left	Cochlear implant not inserted correctly, dysplastic inner ear	Electrode not inside cochlea, basilar turn fenestration and course of electrode passing beside it visible (Figs. 6, 7, 8)
13	72	Female	Right	Carcinoma of temporal bone	Amount of bone erosion is shown, intact ossicular chain is displayed
14	79	Female	Right	Petrosectomy	Intact inner ear and nerve structures are shown, dimensions of cavity are displayed
15	69	Male	Left	Exostosis of external acoustic meatus	Amount of stenosis of the external acoustic meatus is shown
16	22	Male	Left	Post-inflammatory aplasia of lenticular process and stapes apart from base (possible malformation)	Aplasia of structures is shown, normal inner ear and nerve structures are displayed
17	6	Male	Left	Cholesteatoma	Cholesteatoma filling the parts of the tympanic cavity and mastoid and intact ossicular chain are displayed

on the normal side. No history of disease was reported on that side and no disease was found by otomicroscopy, CT, or audiometric measurements. Patients 1 and 2 were examined, to allow the normal anatomy to be compared with the pathological alterations of the anatomy in the other patients. Patients 3–17 had different conditions or post-operative alterations of the middle ear, including cases of malformation, infection, tumour, trauma of the temporal bone and implantation of hearing aids.

Data acquisition was performed by use of a multi-slice CT scanner (GE CT LightSpeed QX/i, GE Medical Systems, Milwaukee, Wis., USA) in the Department of Neuroradiology, Hannover Medical School. CT was obtained with 1.25-mm collimation, exposure duration of 7.8 s and pitch of 3 (140 kV, 40 mA) [21]. Both temporal bones were covered by the original scan. Using a bone-reconstruction algorithm we reconstructed the images to a FOV of 9.6 cm for each side, with a reconstruction interval of 0.3 mm. Voxel dimensions were 0.1875 mm in the *x*-*y* direction and 0.3 mm in the *z* direction. For post-processing the header information was extracted from the resulting Dicom files to make them readable to the software.

Post-processing was performed on an Ultra 80 workstation (Sun Microsystems, Palo Alto, Calif., USA) using the software “3D Slicer” (Surgical Planning Laboratory, Brigham and Women’s Hospital, Harvard Medical School, Boston, Mass., USA; www.slicer.org) [22]. The software allows segmentation of structures in the 2D slices by various techniques. The segmented 2D slices are then put together to form a segmentation volume. This segmentation volume was used to create 3D models using the Visualisation Toolkit (VTK), a software offering a variety of visualisation algorithms to display geometric data.

A segmentation volume of the skull bones was generated by applying a grey-level value of 1,200 as a lower threshold. Noise was reduced by the following algorithm: removal of small islands, an erosion, removal of small islands, and a dilation. In the healthy subject, patient 1, the entire temporal bone and adjacent parts of the skull bones were additionally manually segmented. A second segmentation volume was created by manual segmentation of the three ossicles, the tensor tympani muscle, the inner ear structures, the facial and vestibulo-cochlear nerve, and additional structures depending on the pathology [23]. The two segmentation volumes were merged using the software “mrx” (Surgical Planning Laboratory; splweb.bwh.harvard.edu). With this technique, a single segmentation volume of the dataset was obtained and overlapping of different segmented structures was prevented (see Fig. 1). Three-dimensional models of all the structures were generated using surface rendering, each in a different colour, using a VTK smoothing iteration of 10 for the ossicles, implants and fractures. A VTK smoothing iteration of 20 was applied for the remaining structures. The marching cube algorithm was applied to create the 3D models (see Fig. 2) [24]. The cross-sectional slices were correlated to 3D and virtual endoscopic views by projecting the 2D slice into the 3D model (see Fig. 3). The segmented structures were displayed in the same colours as the 3D models in the segmented cross-sectional slices (see Fig. 1). For the pathological cases 3–17 the relevant cross-sectional slices showing the pathology were correlated to the 3D image. The 3D images were assessed with respect to the quality of display and enhancing of understanding of the individual anatomy in the pathological cases.

Results

As data-analysis was performed retrospectively the impact of 3D visualisation on diagnosis and surgical planning in these cases could not be assessed as a prospective study in a clinical environment. 3D visualisation

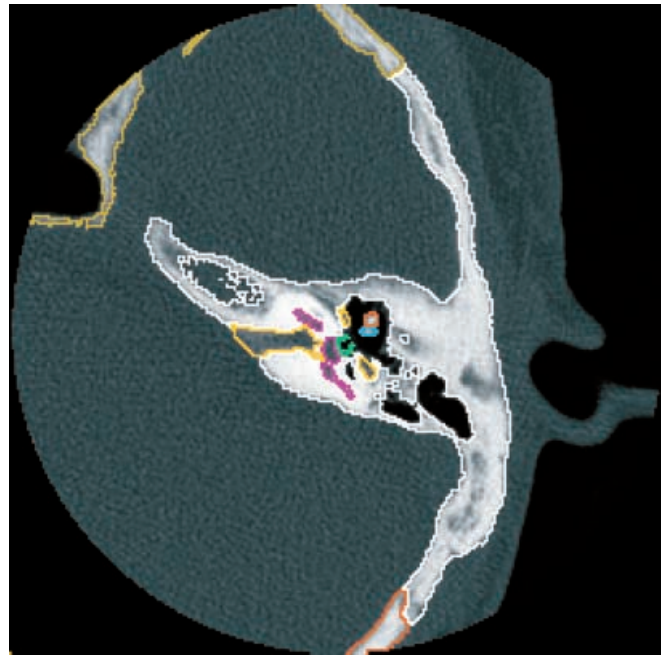


Fig. 1. Normal temporal bone. Axial reconstructed image of temporal bone and adjacent structures showing segmented structures in different colours. Note the ossicles, inner ear and nerve structures (case 1)

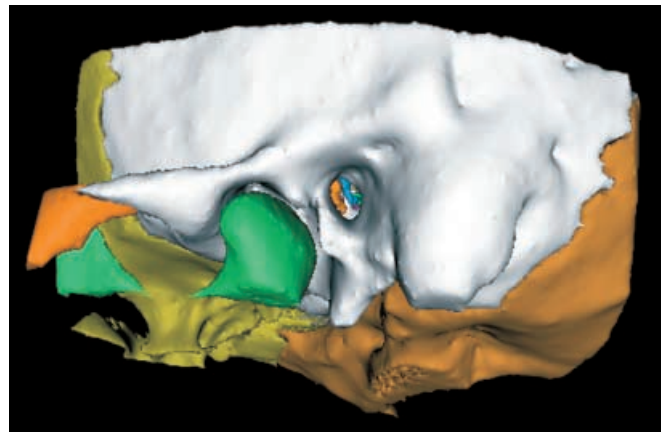


Fig. 2. Normal temporal bone. Lateral view of temporal bone and adjacent structures. Three-dimensional models of the segmented structures are displayed in the same colours as seen in Fig. 1 (case 1)

of all the different structures including the inner ear, and the facial and vestibulo-cochlear nerves, allowed display of the correct anatomy and pathology to high detail in all the cases. The complete ossicular chain was displayed in all cases in which the ossicles were still present. The tensor tympani muscle and pathological structures, such as fracture fragments or fracture gaps, were also displayed. The temporal bone and adjacent parts of the

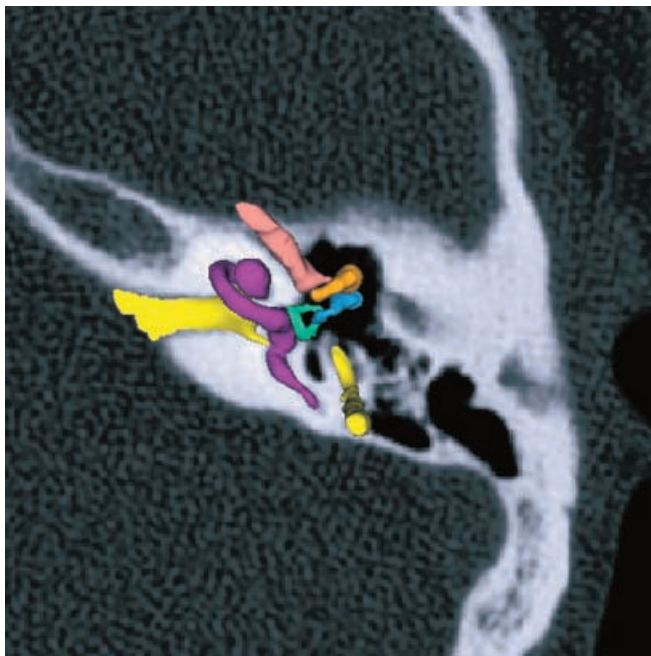


Fig. 3. Normal temporal bone. The axial image of the temporal bone seen in Fig. 1 is correlated to an inferior view of the 3D models of ossicles, inner ear and nerve structures and tensor tympani muscle (case 1)

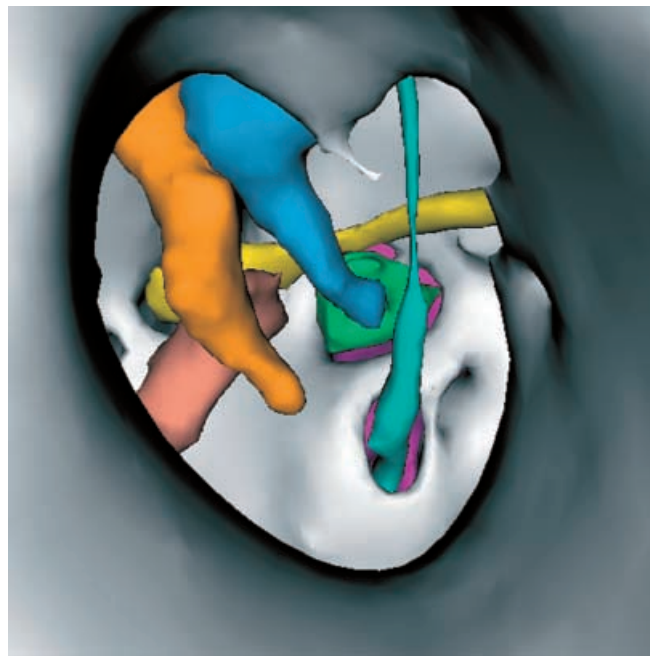


Fig. 4. Cochlear implant. Lateral virtual endoscopic view from the external acoustic meatus towards the tympanic cavity. The electrode is displayed entering the basilar turn fenestration. Normal ossicular chain, tympanic course of facial nerve, tensor tympani muscle and round window niche are displayed (case 11)

other skull bones were visible. In some patients, partial volume effects caused pseudoforamina, that appeared as inadequate defects of the tegmen tympani. In all the cases, correct diagnosis could have been reached using the 2D slices alone.

Post-processing took up to 6 h per case depending on training and the type of pathological condition. This was mainly due to the time-consuming manual segmentation of the various structures and time for merging of datasets and processing of the different models. The 3D “Slicer” software allowed various ways of interaction with the individual 3D models, allowing the user to get the anatomy and pathology presented in a structured way. Models were made completely transparent if they obscured the view of a relevant structure. The individual structures could be translated away from each other, and the opacity for each structure could be set individually. By changing the opacity, the percentage of a light ray being held up by a voxel, a structure could be made transparent. Spatial relationships of obscured structures could thus be revealed. Using surface rendering, real-time navigation was possible. Different colours for each anatomical structure in models and segmented 2D images helped the merging of the 2D and 3D views to a 3D understanding. Stereoscopic views could be created where they enhanced 3D perception.

Correlation of the 2D images to the 3D models was possible for axial, coronal and sagittal images in all the cases. Stacking up the 2D images in order to reach a 3D

understanding of the individual anatomy was thus made easier. Such enhancement can be especially helpful for cases of malformation where the observer could not rely on the usual anatomic landmarks due to aplasia or dysplasia of the structure. Furthermore, correlation of 2D images to 3D visualisation helped to detect the distinct spatial relationship of different structures.

For instance, the course of the electrodes could be followed and displayed within the cochlea in the cases of cochlear implants (see Figs. 4, 5). In patient 12, the course of the electrode running beside the basilar turn fenestration was displayed (see Figs. 6, 7, 8). The continuity of the ossicular chain connecting the tympanic membrane and the oval window could be assessed in patient 9 who had an ossicular prosthesis (see Figs. 9, 10). In patient 8, it could be shown that the prosthesis did not connect to the inner ear. In the cases of trauma the fracture course was more easily visualised in the 2D images. Correlation of the fracture course and the damaged cochlea or the dislocated ossicles was displayed (see Figs. 11, 12, 13, 14). In patient 7 impingement of a fracture fragment causing dislocation of both the incudomalleolar and incudostapedial joint was displayed. The amount of bone destruction could be shown in a case of petrous bone carcinoma along with a still-intact ossicular chain. The localisation of damaged areas in relation to the tympanic cavity could be assessed.

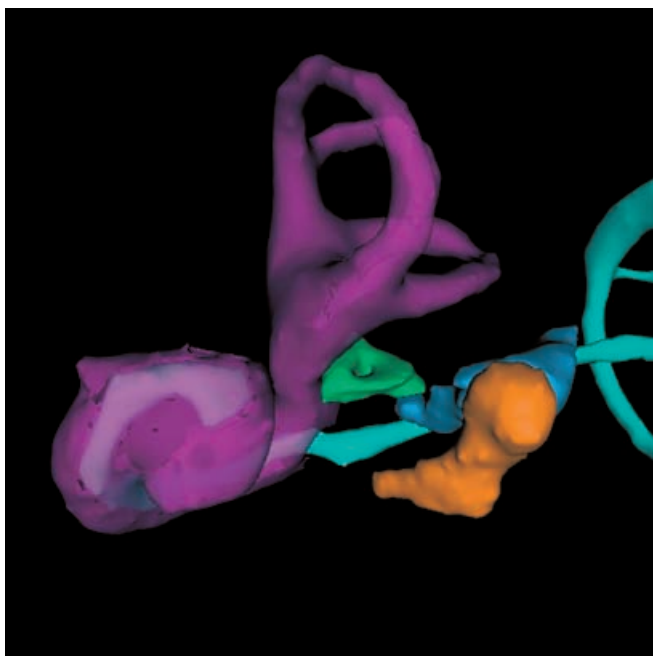


Fig. 5. Cochlear implant. Anterior view shows electrode entering inner ear and course of electrode inside cochlea (case 11)

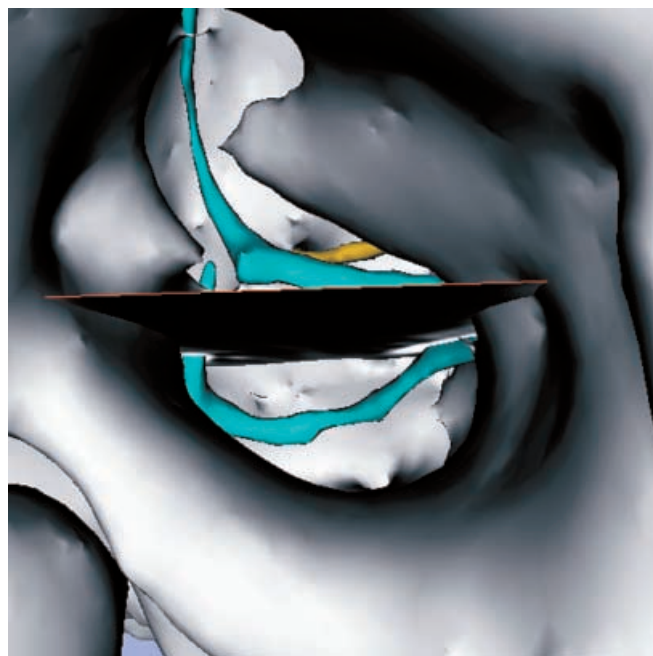


Fig. 7. Cochlear implant. Axial image as seen in Fig. 6 correlated to lateral virtual endoscopic view (case 12)

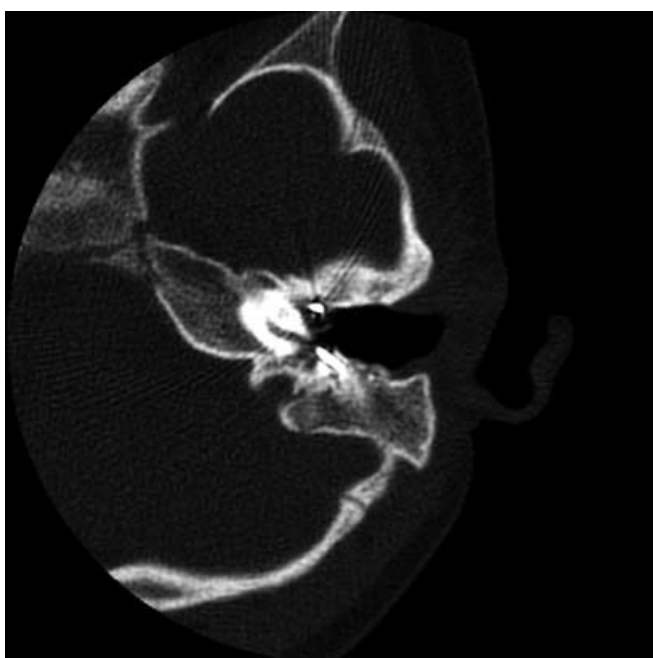


Fig. 6. Cochlear implant. Axial image shows basilar turn fenestration (case 12)

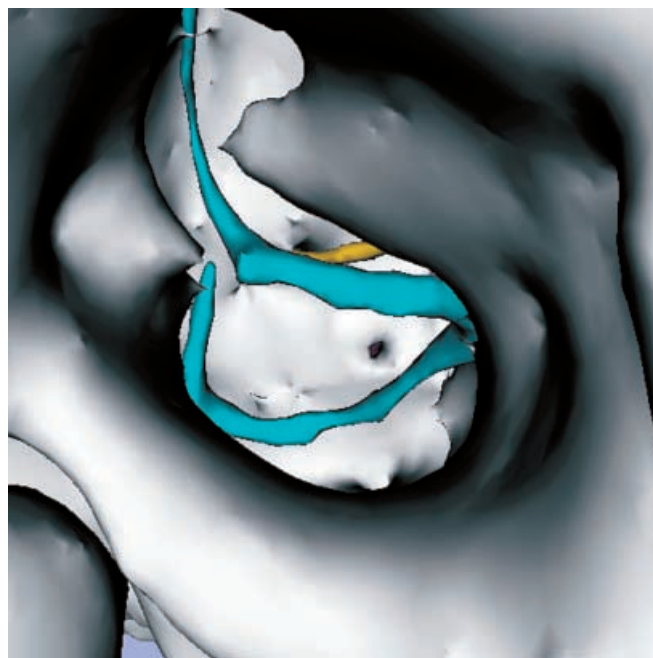


Fig. 8. Cochlear implant. Lateral virtual endoscopic view as seen in Fig. 7 displays basilar turn fenestration and course of electrode passing beside it (case 12)

Discussion

The patients investigated in this study present a selection of cases of middle-ear conditions that might appear in any neuroradiological centre. In order to show

the feasibility of the method for clinical and teaching purposes, we concentrated more on the variety of relevant cases than on the number of them. Studies showing the clinical benefit of 3D visualisation of the temporal bone for certain indications have already been

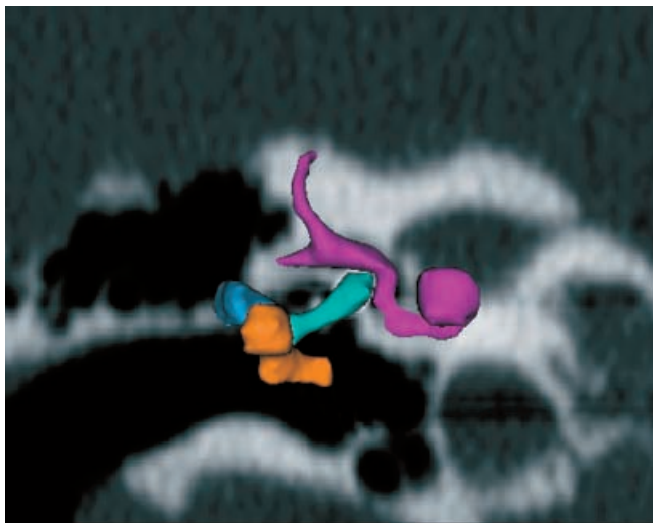


Fig. 9. Stapes prosthesis. Anterior view of 3D models correlated to coronal slice. Note the continuity of ossicular chain (case 9)

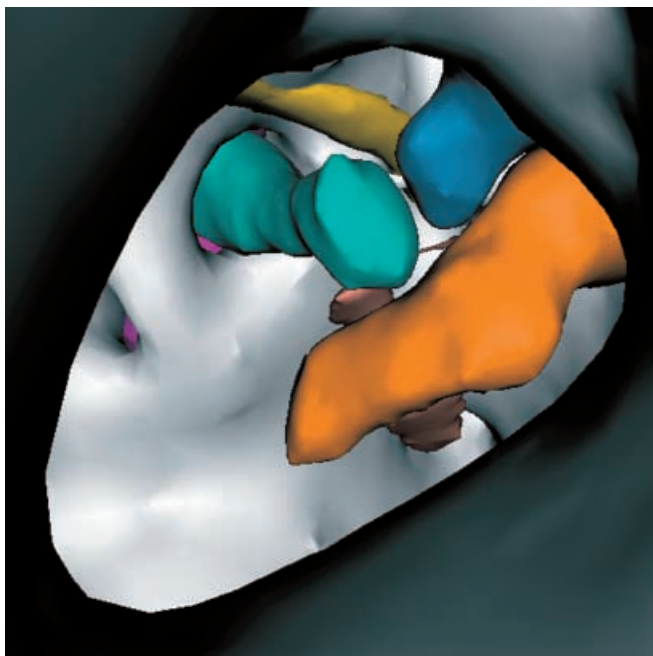


Fig. 10. Stapes prosthesis. Lateral virtual endoscopic view from the external acoustic meatus. Ossicular chain, course of facial nerve, tensor tympani muscle and round window niche are displayed. Note the continuity of ossicular chain (case 9)

presented [4, 15, 19, 20]. We were able to confirm that 3D visualisation is beneficial in gaining a 3D understanding of the patient's anatomy and pathological condition. An approach to temporal-bone imaging is presented in this study that adds this diagnostic benefit to that of conventional CT images, that often show higher detail.

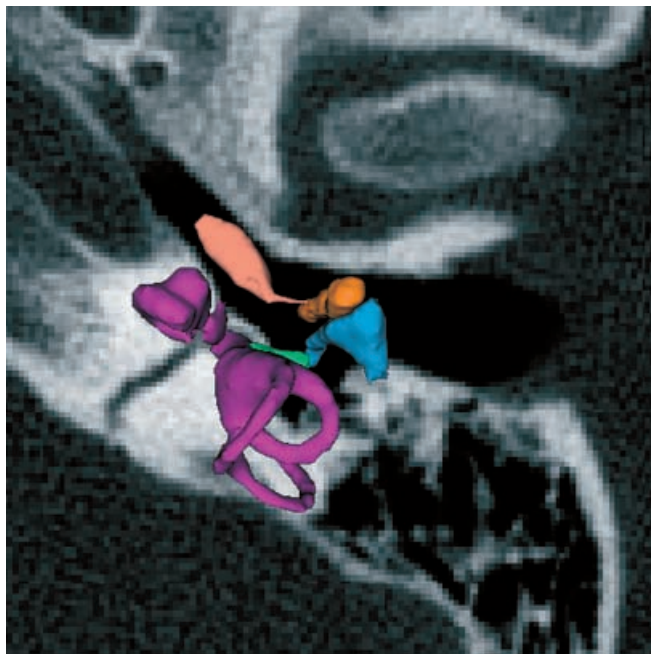


Fig. 11. Fracture of temporal bone. Superior view of 3D models correlated to axial slice. The course of the fracture running through the cochlea is shown (case 5)

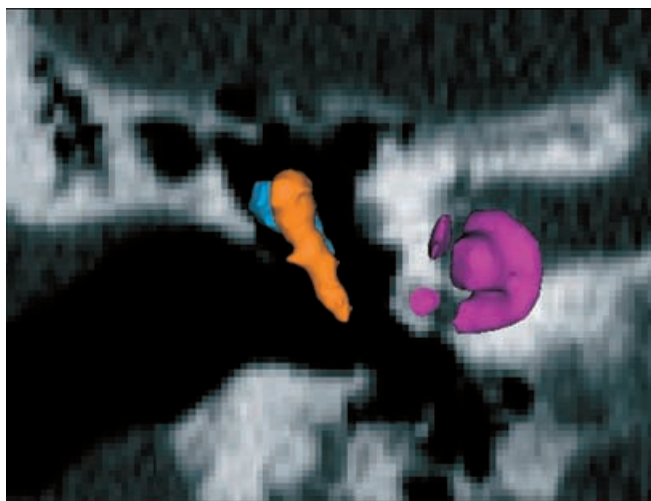


Fig. 12. Fracture of temporal bone. Anterior view of 3D models correlated to coronal slice. The course of the fracture running through the cochlea is shown (case 5)

Furthermore, routine low-dosage protocol using multi-slice CT was used, ensuring that no additional dosage would be applied to the patient and that the datasets met the current radiological status in a clinical environment. Magnetic resonance imaging (MRI) allows enhanced 3D visualisation for a different clinical focus, especially when the inner ear has to be evaluated [19, 25, 26]. With MRI the different portions of the facial and



Fig. 13. Dislocation of incudomalleolar joint. Axial image shows dislocation of incudomalleolar joint and fracture of the temporal bone (case 6)

vestibulo-cochlear nerve can be depicted to very high detail [27]. CT, however, is the method used for assessment of the bone structures. In the future, registration of CT and MRI data might enhance the possibility of determining adjacent structures such as the nerve structures, inner ear, soft-tissue masses and tumours.

Post-processing was performed using surface rendering, as this is the algorithm most widely available, and it enables real-time navigation even on less-powerful computers. The volume rendering algorithm may allow better display of smaller structures. The quality of display of the normal anatomy and pathology using manual segmentation is still superior to automated segmentation algorithms. Thresholding can be standardised easily, but has shortcomings in the case of simultaneous 3D visualisation of structures of different attenuation values [4, 5]. Automated segmentation algorithms based on elastic registration, currently being developed and assessed for clinical use, may significantly reduce post-processing time while allowing precise segmentation. Minimising post-processing time is of paramount importance in a clinical setting. Although it

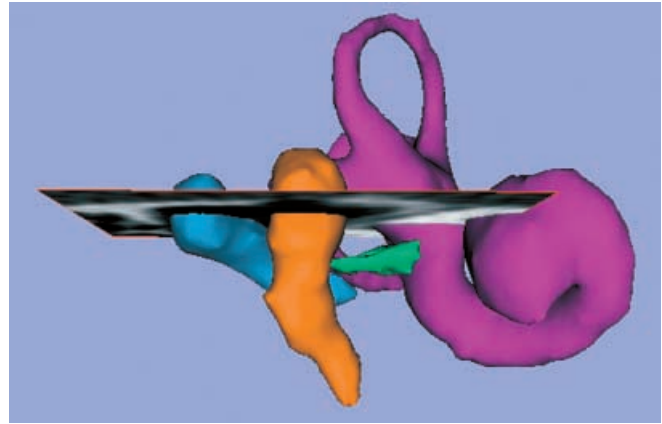


Fig. 14. Dislocation of incudomalleolar joint. Axial image as seen in Fig. 13 is correlated to anterior view of 3D models of ossicular chain and inner ear. The amount of dislocation is shown (case 6)

is the main cost-factor, one should keep in mind that with the advent of more-powerful computers and automated post-processing algorithms this is likely to change.

Implementation of methods to correlate 2D and 3D images to post-processing-software will be useful for radiological diagnosis, surgical planning, and teaching.

By combining both modalities, the one that is better suited to displaying a certain pathological condition can be chosen without the loss of simultaneously visible valuable information shown by the other modality. Furthermore, it is easier for the clinician to integrate the 3D views into the system of anatomic landmarks in the 2D slices used for orientation when appraising the images. The radiologists' system is more likely to be based on the axial images, whereas the otorhinolaryngologists' system is more likely to be based on the coronal images, as this is more similar to their approach to the anatomy during surgery. Based on correlation of the modalities, demonstration of cases to another speciality could therefore be optimised. Cases of correlated individual 2D and 3D anatomy in pathological conditions will facilitate the learning process and can be used as a reference. The potential of this method for surgical planning is highlighted by the opportunity of using the more-accurate 2D images for measurement and planning without having to resign from maintaining a 3D overview.

References

1. Ali QM, Ulrich C, Becker H (1993) Three-dimensional CT of the middle ear and adjacent structures. *Neuroradiology* 35:238–241
2. Howard JD, Elster AD, May JS (1990) Temporal bone: three-dimensional CT. I. Normal anatomy, techniques, and limitations. *Radiology* 177:421–425
3. Howard JD, Elster AD, May JS (1990) Temporal bone: three-dimensional CT. II. Pathologic alterations. *Radiology* 177:427–430

4. Schubert O, Sartor K, Forsting M, Reisser C (1996) Three-dimensional computed display of otosurgical operation sites by spiral CT. *Neuroradiology* 38:663–668
5. Reisser C, Schubert O, Forsting M, Sartor K (1996) Anatomy of the temporal bone: detailed three-dimensional display based on image data from high-resolution helical CT: a preliminary report. *Am J Otol* 17:473–479
6. Hermans R, Marchal G, Feenstra L, Baert AL (1995) Spiral CT of the temporal bone: value of image reconstruction at submillimetric table increments. *Neuroradiology* 37:150–154
7. Isono M, Murata K, Aiba K, Miyashita H, Tanaka H, Ishikawa M (1997) Minute findings of inner ear anomalies by three-dimensional CT scanning. *Int J Pediatr Otorhinolaryngol* 42:41–53
8. Leuwer R, Schubert R, Siepmann (1993) Three-dimensional reconstruction of a high-resolution MR-tomography of the inner ear. *Laryngorhinootologie* 72:288–290
9. Dammann F, Bode A, Schwaderer E, Schaich M, Heuschmid M, Maassen MM (2001) Computer-aided surgical planning for implantation of hearing aids based on CT data in a VR environment. *Radiographics* 21:183–190
10. Himi T, Kataura A, Sakata M, Odawara Y, Satoh J, Sawaiishi M (1996) Three-dimensional imaging of the temporal-bone using a helical CT scan and its application in patients with cochlear implantation. *ORL J Otorhinolaryngol Relat Spec* 58:298–300
11. Frankenthaler RP, Moharir V, Kikinis R, van Kipshagen P, Jolesz F, Umans C, Fried MP (1998) Virtual otoscopy. *Otolaryngol Clin North Am*. 31:383–392
12. Shibata T, Nagano T (1996) Applying very high resolution microfocus X-ray CT and 3-D reconstruction to the human auditory apparatus. *Nat Med* 2:933–935
13. Tomandl BF, Hastreiter P, Eberhardt KEW, Rezk-Salama C, Naraghi R, Greess H, Nissen U, Huk WJ (2000) Virtual labyrinthoscopy: visualization of the inner ear with interactive direct volume rendering. *Radiographics* 20:547–558
14. Seemann MD, Seemann O, Bonél H, Suckfüll M, Englmeier KH, Naumann A, Allen CM, Reiser MF (1999) Evaluation of the middle and inner ear structures: comparison of hybrid rendering, virtual endoscopy and axial 2D source images. *Eur Radiol* 9:1851–1858
15. Klingenbiel R, Bauknecht HC, Lehmann R, Rogalla P, Werbs M, Behrbohm H, Kaschke O (2000) Virtual otoscopy – technique indications and initial experience with multi-slice spiral CT. *Fortschr Roentgenstr* 172:872–878
16. Himi T, Sakata M, Shintani T, Mitsuzawa H, Kamagata M, Satoh J, Sugimoto H (2000) Middle ear imaging using virtual endoscopy and its application in patients with ossicular chain anomaly. *ORL J Otorhinolaryngol Relat Spec* 62:316–320
17. Boor S, Maurer J, Mann W, Stoeter P (2000) Virtual endoscopy of the inner ear and the auditory canal. *Neuroradiology* 42:543–547
18. Pozzi Mucelli R, Morra A, Calgaro A, Cova M, Cioffi V (1997) Virtual endoscopy with computed tomography of the anatomical structures of the middle ear. *Radiol Med (Torino)* 94:440–446
19. Neri E, Caramella D, Cosottini M, Zampa V, Jackson A, Berrettini S, Sellari-Franceschini S, Bartolozzi C (2000) High-resolution magnetic resonance and volume rendering of the labyrinth. *Eur Radiol* 10:114–118
20. Jahrsdoerfer RA, Garcia ET, Yeakley JW, Jacobson JT (1993) Surface contour three-dimensional imaging in congenital aural atresia. *Arch Otolaryngol Head Neck Surg* 119:95–99
21. Hu H (1999) Multi-slice helical CT: scan and reconstruction. *Med Phys* 26:5–18
22. Gering D (1999) A system for surgical planning and guidance using image fusion and interventional MR (Master's thesis). Massachusetts Institute of Technology, Boston, Mass
23. Fried MP, Moharir VM, Shinmoto H, Alyassin AM, Lorensen WE, Hsu L, Kikinis R (1999) Virtual laryngoscopy. *Ann Otol Rhinol Laryngol* 108:221–226
24. Lorensen W, Cline H (1987) Marching cubes: a high resolution 3D surface construction algorithm. *Comput Graph* 21:163–169
25. Melhem ER, Shakir H, Bakthavachalam S, MacDonald CB, Gira J, Caruthers SD, Jara H (1998) Inner ear volumetric measurements using high-resolution 3D T2-weighted fast spin-echo MR imaging: initial experiences in healthy subjects. *Am J Neuroradiol* 19:1819–1822
26. Diamantopoulos II, Ludman CN, Martel AL, O'Donoghue GM (1999) Magnetic resonance imaging virtual endoscopy of the labyrinth. *Am J Otol* 20:748–751
27. Sartoretti-Schefer S, Kollias S, Wichmann W, Valavanis A (1998) T2-weighted three-dimensional fast spin-echo MR in inflammatory peripheral facial nerve palsy. *Am J Neuroradiol* 19:491–495